

Specular beamforming and refraction correction improve ultrasound imaging of the bone cortex geometry in-vivo

Amadou S. DIA¹ Quentin GRIMAL¹ Guillaume RENAUD^{1,2}

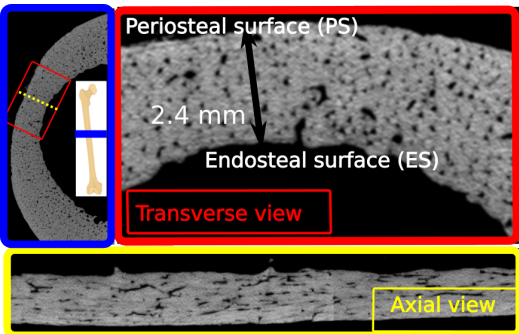
¹Sorbonne Université, INSERM, CNRS, Laboratoire d'Imagerie Biomedicale, LIB, F-75006 Paris, France,

²Department of Imaging Physics, Delft University of Technology, The Netherlands

IEEE/IUS, International Ultrasound Symposium 2023

Cortical thickness and wave-speed can be estimated using ultrasound imaging

Cortical thickness and microstructure can help assess bone health.

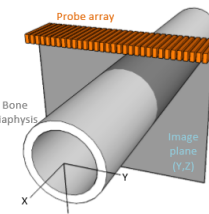


Ultrasound imaging can be used to estimate:

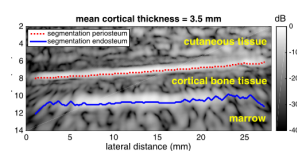
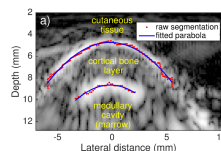
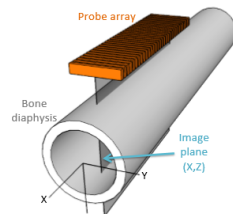
- Cortical thickness
- Wave-speed and anisotropy parameters in cortical bone

Synthetic focusing imaging

a) Configuration for a transverse image



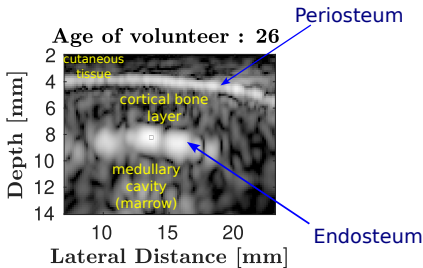
b) Configuration for a longitudinal image



[Renaud et al., Phys. Med. Biol., 2018
Renaud et al., Phys. Med. Biol., 2020]

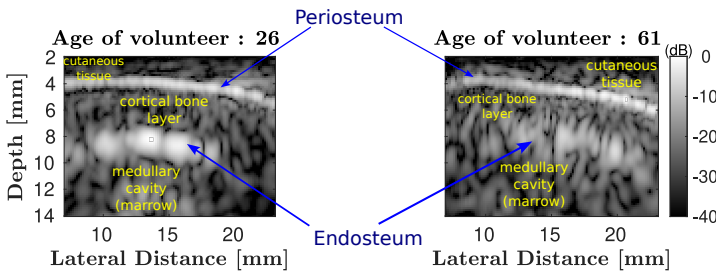
The present study focuses on the transverse plane.

As microstructure degrades, contrast of bone internal surface diminishes



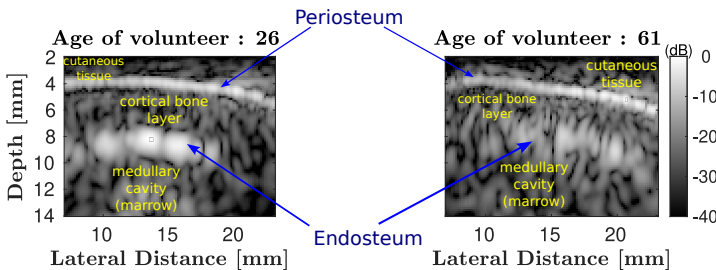
A “high-quality” ultrasound bone image would optimally show bright external (periosteum) and internal (endosteum) surfaces.

As microstructure degrades, contrast of bone internal surface diminishes



A “high-quality” ultrasound bone image would optimally show bright external (periosteum) and internal (endosteum) surfaces.

As microstructure degrades, contrast of bone internal surface diminishes



A “high-quality” ultrasound bone image would optimally show bright external (periosteum) and internal (endosteum) surfaces.

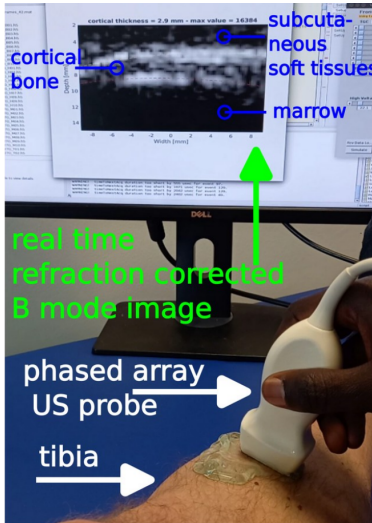
Problematic: As intra-cortical pore density or pore diameter increases, speckle intensity generated by cortical bone tissue increases.

[Dia et al. Ultrasonics 2023]

Objective

Develop an image reconstruction technique that would enhance visibility of surfaces of the bone cortex.

In-vivo data acquisitions



Programmable ultrasound system :
Vantage research ultrasound scanner Verasonics

In-house real-time intra-osseous image reconstruction code (BoneImage)

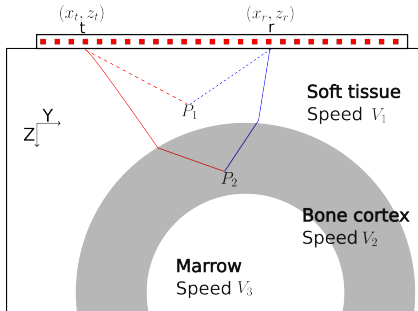
Probe characteristics

- Phased array, model: P4-1, Philips ATL
- Center frequency: 2.5 MHz, BW=80%
- Pitch = 295 μm
- 96 elements

In vivo data are obtained during a study on healthy volunteers.

Synthetic Aperture (Single Element Transmissions) acquisitions in the transverse plane at tibial mid-shaft.

In-house intra-osseous image reconstruction code (BoneImage)



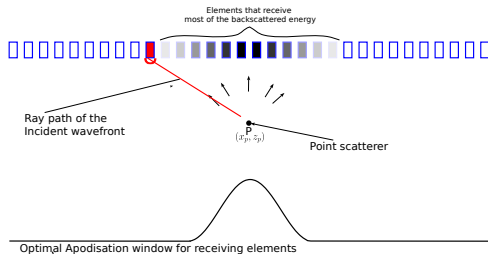
Speed of sound in cortical bone is $2\times$ higher than in soft tissues.

Round-trip time of flights from an element of the probe to a point in the medium are computed taking into account refraction at bone - soft-tissues interface.

Like conventional delay-and-sum, technique most suited for point-diffractor imaging

[Renaud et al., *Phys. Med. Biol.*, 2018
Renaud et al., *Phys. Med. Biol.*, 2020]

Specular interface back-scatters ultrasound in a specific direction (Snell's law)

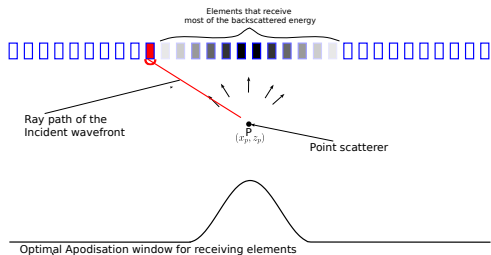


Diffuse scattering : No directivity

The choice of the receive sub-aperture is only governed by the directivity of the elements.

This is the hypothesis of Delay And Sum (DAS) beamforming.

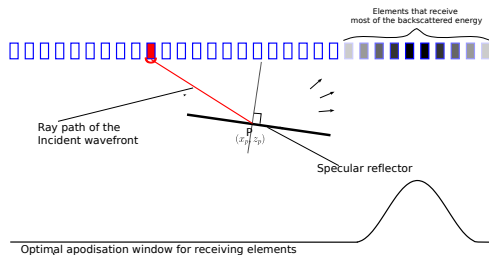
Specular interface back-scatters ultrasound in a specific direction (Snell's law)



Diffuse scattering : No directivity

The choice of the receive sub-aperture is only governed by the directivity of the elements.

This is the hypothesis of Delay And Sum (DAS) beamforming.

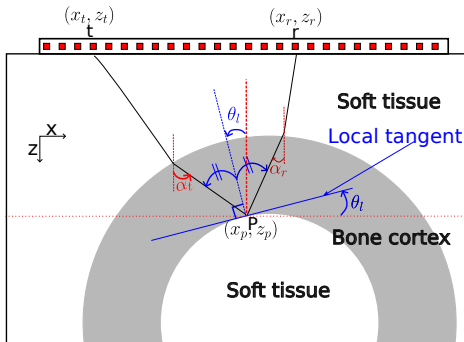


Specular scattering : Propagation direction of backscattered signal depends on incident angle and orientation of the specular interface.

An adaptive receive sub-aperture can be used.

*Malamal et Panicker Biomed. Phys. Eng. Express 2023,
Nagaoka et al. J Med Ultrasonics 2020,
Rodriguez-Molares et al. 2017,
Bandaru et al. IEEE 2016*

Transform to the basis of receive and transmit angles for each pixel



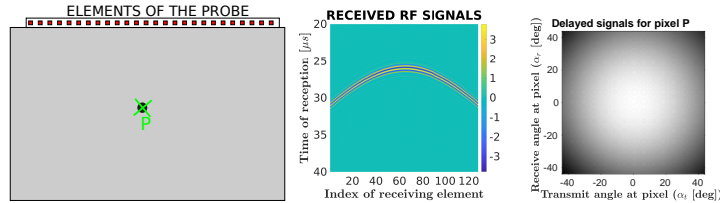
We move from the basis of receive and transmit element (t, r) to the basis of receive and transmit angles (α_t, α_r) .

In this basis, **Snell's law for specular reflection** is written :

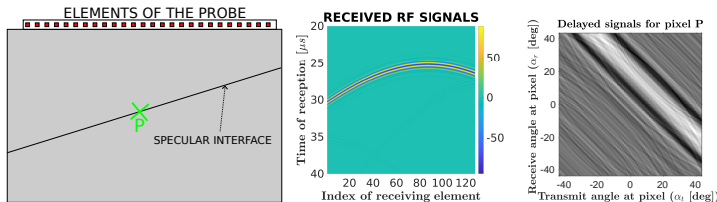
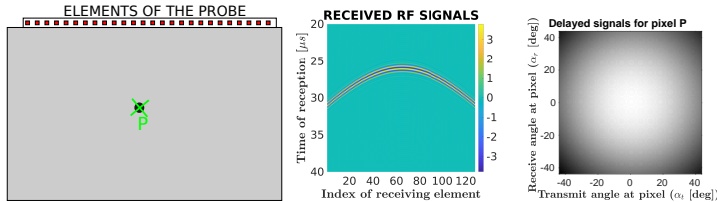
$$\alpha_r + \alpha_t - 2 \cdot \theta_l = 0$$

The local specular angle θ_l is unknown.

Received signal from a specular object have specific signature in the basis of receive and transmit angles



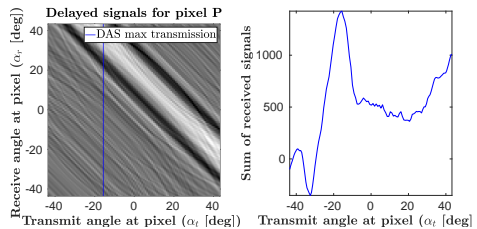
Received signal from a specular object have specific signature in the basis of receive and transmit angles



Summation of echo signals exploiting the specular reflection by a flat tilted interface

Classical DAS beamforming:

For each transmission, sum all delayed signals
within a receive sub-aperture



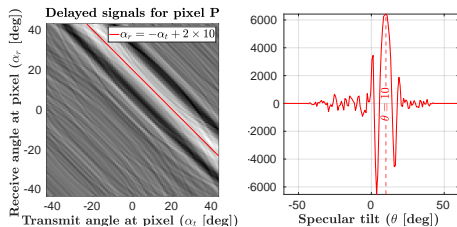
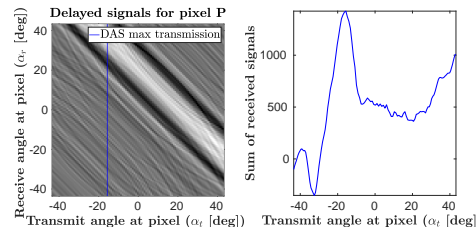
Summation of echo signals exploiting the specular reflection by a flat tilted interface

Classical DAS beamforming:

For each transmission, sum all delayed signals within a receive sub-aperture

Specular transform (*Rodriguez-Molares et al. 2017*):
Sum all delayed signals that satisfy specular reflection for a candidate surface orientation θ .

$$f(P, \theta) = \sum_{t=1}^{N_T} \mathbf{S}_{rf}(\tau_p(t, r), \alpha_r, \alpha_t)|_{\alpha_r + \alpha_t = 2\theta}$$



Estimation of the index of specularity and inclination of specular objects

The normalized cross correlation (\star) of the specular transform $f(P, \theta)$ with a model $h(P, \theta)$ gives:

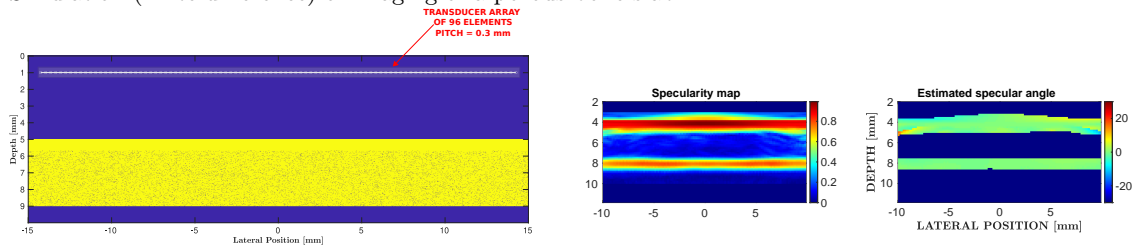
- The index of specularity : probability of finding a specular object at P.

$$\Psi(P) = \max \{f(P, \theta) \star h(P, \theta)\}$$

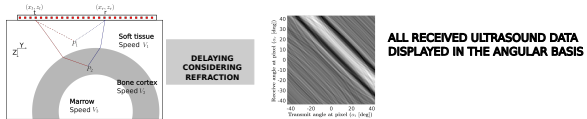
- The orientation of the specular object lying at point P.

$$\tilde{\theta}(P) = \arg \max \{f(P, \theta) \star h(P, \theta)\}$$

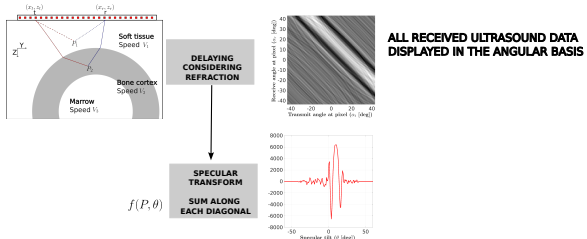
Simulation (finite difference) of imaging of a porous bone slab



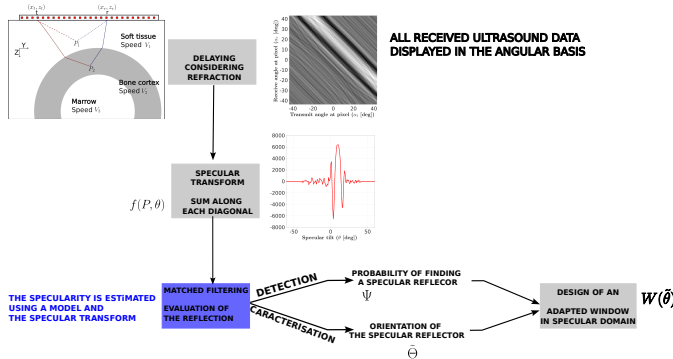
Synopsis of specular beamforming applied to the bone cortex.



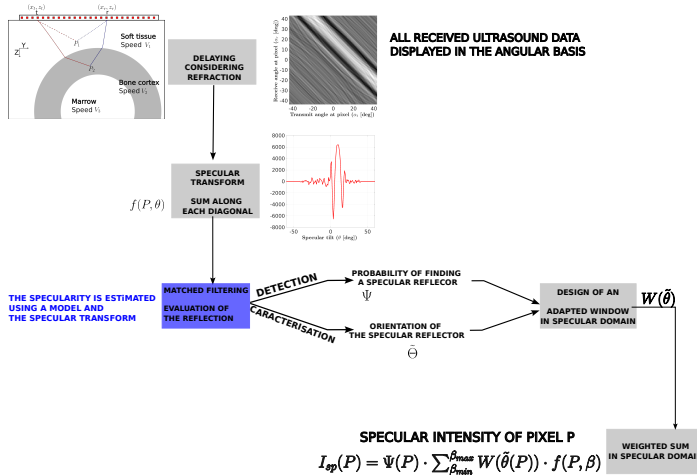
Synopsis of specular beamforming applied to the bone cortex.



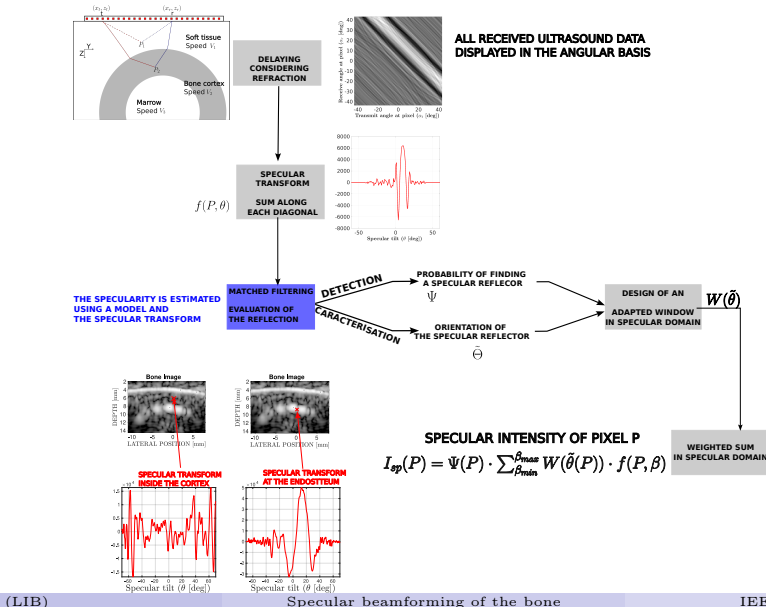
Synopsis of specular beamforming applied to the bone cortex.



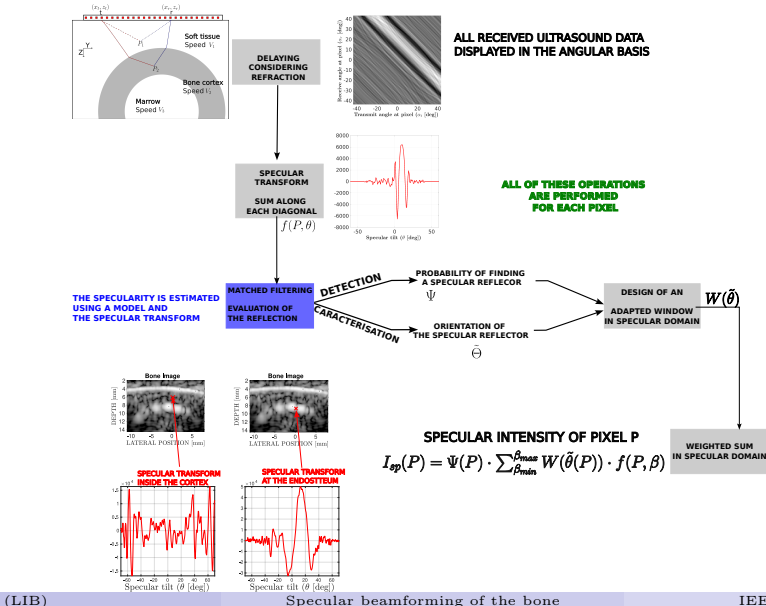
Synopsis of specular beamforming applied to the bone cortex.



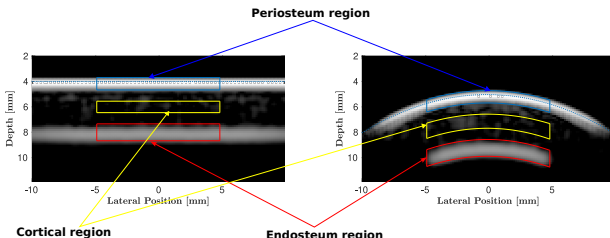
Synopsis of specular beamforming applied to the bone cortex.



Synopsis of specular beamforming applied to the bone cortex.



Quantification of endosteal interface visibility



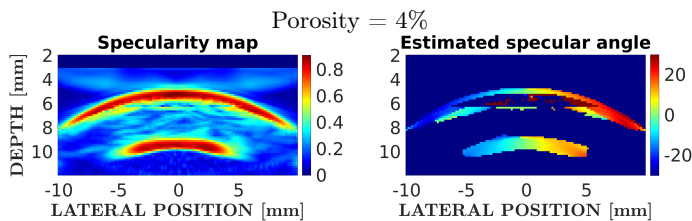
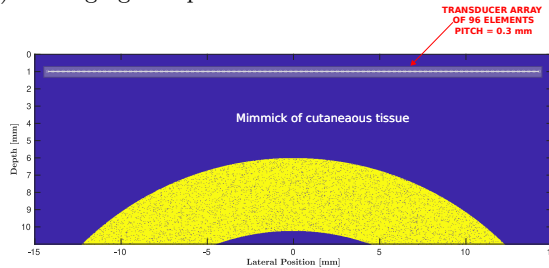
$$C_{EP} = \frac{\text{ENDOSTEUM}}{\text{PERIOSTEUM}}$$
$$C_{EI} = \frac{\text{ENDOSTEUM}}{\text{INNER CORTEX}}$$

Metrics are expressed in dB.

We want to increase C_{EI} value while maintaining constant C_{EP} value.

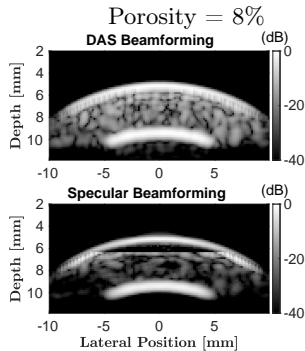
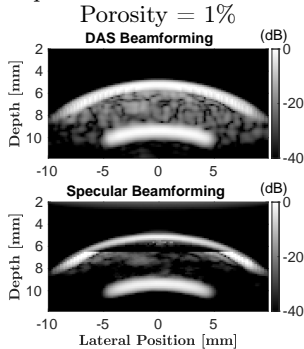
Simulation results: specularity and tilt maps give information on the geometry of the bone

Simulation (finite difference) of imaging of a porous bone slab



Simulation results: Specular beamforming increases endosteum visualisation

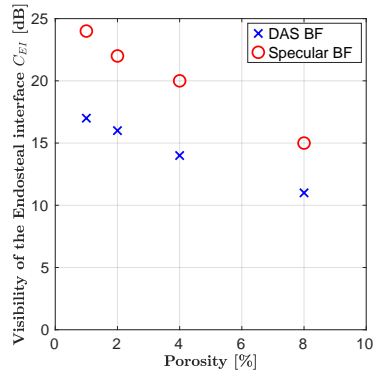
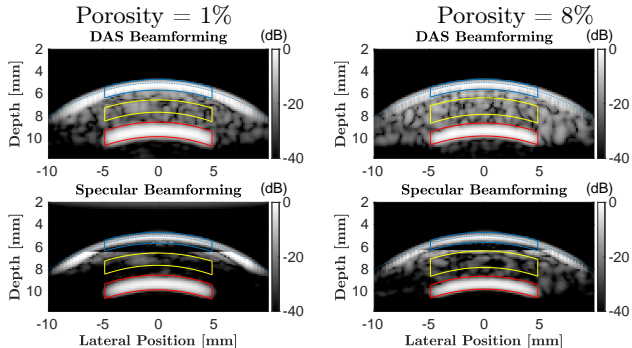
For porosities of 1 and 8 %



Compared to DAS, specular beamforming increases endosteum visualisation by 6 dB.

Simulation results: Specular beamforming increases endosteum visualisation

For porosities of 1 and 8 %



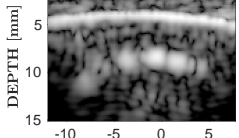
Compared to DAS, specular beamforming increases endosteum visualisation by 6 dB.

In-Vivo results

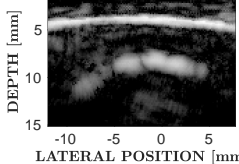
Refraction-corrected
DAS Beamforming

Age of Volunteer: 26

$$C_{EI}=12 \text{ dB}, C_{EP}=-7.2 \text{ dB}$$

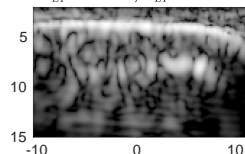


$$C_{EI}=19 \text{ dB}, C_{EP}=-7.3 \text{ dB}$$

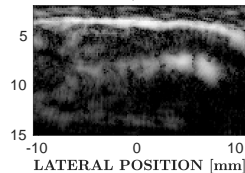


Age of Volunteer: 28

$$C_{EI}=7.1 \text{ dB}, C_{EP}=-9.3 \text{ dB}$$

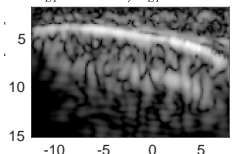


$$C_{EI}=11 \text{ dB}, C_{EP}=-9.3 \text{ dB}$$

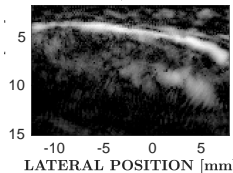


Age of Volunteer: 61

$$C_{EI}=5.5 \text{ dB}, C_{EP}=-11 \text{ dB}$$



$$C_{EI}=9 \text{ dB}, C_{EP}=-11 \text{ dB}$$

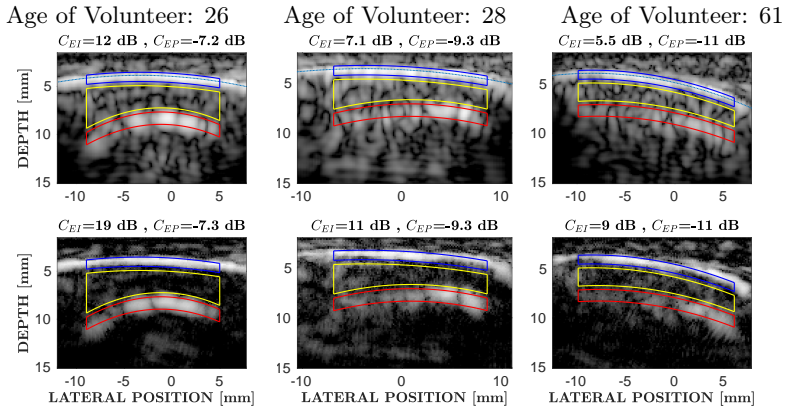


Refraction-corrected
Specular Beamforming

Images are log compressed and displayed with a dynamic range of 40 dB.

In-Vivo results

Refraction-corrected
DAS Beamforming



Images are log compressed and displayed with a dynamic range of 40 dB.

The visibility of the endosteal interface increases by 3 to 7 dB.

Summary

Visualization of the intra-osseous anatomy is enhanced by 3 to 7 dB when combining specular beamforming and refraction correction algorithms.

Conclusion

Summary

Visualization of the intra-osseous anatomy is enhanced by 3 to 7 dB when combining specular beamforming and refraction correction algorithms.

Perspectives

- Application to more cases including pathological cases

Conclusion

Summary

Visualization of the intra-osseous anatomy is enhanced by 3 to 7 dB when combining specular beamforming and refraction correction algorithms.

Perspectives

- Application to more cases including pathological cases
- Real time.

Conclusion

Summary

Visualization of the intra-osseous anatomy is enhanced by 3 to 7 dB when combining specular beamforming and refraction correction algorithms.

Perspectives

- Application to more cases including pathological cases
- Real time.
- Specularity map sufficient to represent anatomical image of the cortex.

Conclusion

Summary

Visualization of the intra-osseous anatomy is enhanced by 3 to 7 dB when combining specular beamforming and refraction correction algorithms.

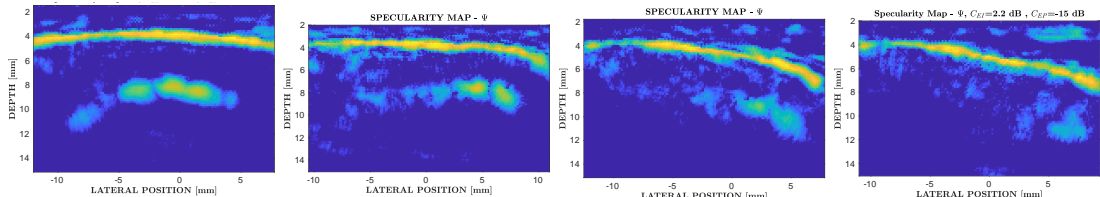
Perspectives

- Application to more cases including pathological cases
- Real time.
- Specularity map sufficient to represent anatomical image of the cortex.
- Parametric imaging of the bone: specularity of the medium could be used to evaluate the rugosity of cortical bone surfaces which is an indicator of bone health.

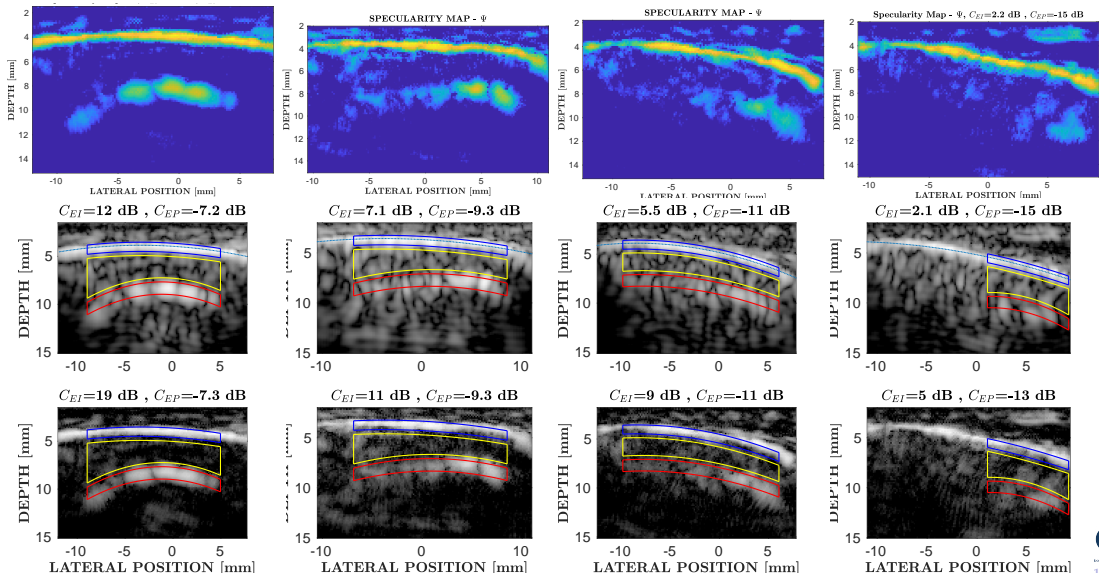
The end

Thank you for your attention. Do you have any questions?

Backup : In-Vivo results



Backup : In-Vivo results



(LIB)

Specular beamforming of the bone

IEEE/IUS 2023